ENDOMETRIOSIS

Neuropeptide S receptor 1 is a nonhormonal treatment target in endometriosis

Thomas T. Tapmeier[1,2*†], Nilufer Rahmioglu[1,3†], Jianghai Lin[1,4†], Bianca De Leo[5], Maik Obendorf[5], Muthuswamy Raveendran[6], Oliver M. Fischer[5], Cemsel Bafligil[7], Manman Guo[7], Ronald Alan Harris[6], Holger Hess-Stumpp[5], Alexis Laux-Biehlmann[5], Ernesto Lowy[3], Gerton Lunter[8], Jessica Malzahn[7], Nicholas G. Martin[9], Fernando O. Martinez[10], Sanjiv Manek[11], Stefanie Mesch[5], Grant W. Montgomery[9,12], Andrew P. Morris[3,13], Jens Nagel[5], Heather A. Simmons[14], Denise Brocklebank[3], Catherine Shang[1], Susan Treloar[9], Graham Wells[7], Christian M. Becker[1], Udo Oppermann[7], Thomas M. Zollner[5], Stephen H. Kennedy[1], Joseph W. Kemnitz[14,15], Jeffrey Rogers[6,14,16], Krina T. Zondervan[1,3*]

Endometriosis is a common chronic inflammatory condition causing pelvic pain and infertility in women, with limited treatment options and 50% heritability. We leveraged genetic analyses in two species with spontaneous endometriosis, humans and the rhesus macaque, to uncover treatment targets. We sequenced DNA from 32 human families contributing to a genetic linkage signal on chromosome 7p13-15 and observed significant overrepresentation of predicted deleterious low-frequency coding variants in *NPSR1*, the gene encoding neuropeptide S receptor 1, in cases (predominantly stage III/IV) versus controls ($P = 7.8 \times 10^{-4}$). Significant linkage to the region orthologous to human 7p13-15 was replicated in a pedigree of 849 rhesus macaques ($P = 0.0095$). Targeted association analyses in 3194 surgically confirmed, unrelated cases and 7060 controls revealed that a common insertion/deletion variant, rs142885915, was significantly associated with stage III/IV endometriosis ($P = 5.2 \times 10^{-5}$; odds ratio, 1.23; 95% CI, 1.09 to 1.39). Immunohistochemistry, qRT-PCR, and flow cytometry experiments demonstrated that NPSR1 was expressed in glandular epithelium from eutopic and ectopic endometrium, and on monocytes in peritoneal fluid. The NPSR1 inhibitor SHA 68R blocked NPSR1-mediated signaling, proinflammatory TNF-α release, and monocyte chemotaxis in vitro ($P < 0.01$), and led to a significant reduction of inflammatory cell infiltrate and abdominal pain ($P < 0.05$) in a mouse model of peritoneal inflammation as well as in a mouse model of endometriosis. We conclude that the NPSR1/NPS system is a genetically validated, nonhormonal target for the treatment of endometriosis with likely increased relevance to stage III/IV disease.

INTRODUCTION

Endometriosis, the growth of endometrial-like tissue outside the uterus, is a common, chronic, estrogen-dependent inflammatory condition affecting an estimated 5 to 10% of women (190 million globally) in their reproductive years (*1*). Lesions are primarily located on pelvic organs, and the disease often causes intense pelvic pain exacerbated by menstruation and reduced fertility. The total annual societal cost of endometriosis-associated symptoms has been estimated at US $50 billion in the United States alone, incurring direct health care costs similar to type 2 diabetes (*2*).

Endometriosis is usually classified surgically according to the revised American Society of Reproductive Medicine (ASRM) stage I to IV classification system (*3*). However, surgical stage correlates poorly with pelvic pain severity (*4*). The pain experienced as the predominant symptom of endometriosis is likely caused by chronic localized inflammation (*5*), even after lesions have been removed or destroyed (*6*), with peripheral and central nervous sensitization contributing to the overall pathophysiology (*7*). Current treatment options are limited to invasive surgical procedures to remove or destroy lesions, or hormonal treatments that can have marked side effects (*8*).

The causes of endometriosis remain largely elusive, but heritability has been estimated at around 50% (*9*). Here, we first used genetic analyses in human family- and population–based studies, complemented by a study of a large pedigree of rhesus macaques (*Macaca mulatta*) with spontaneous endometriosis, to identify associations with low-frequency [minor allele frequency (MAF) < 0.05] and common variants in neuropeptide S (NPS) receptor 1 (*NPSR1*) and subsequently conducted both in vitro and in vivo target validation and inhibition studies of NPSR1 to demonstrate its promise as a treatment target for endometriosis.

[1]Oxford Endometriosis CaRe Centre, Nuffield Department of Women's & Reproductive Health, University of Oxford, Women's Centre, John Radcliffe Hospital, Oxford OX3 9DU, UK. [2]Department of Obstetrics and Gynaecology, Monash University, Clayton, Victoria 3168, Australia. [3]Wellcome Centre for Human Genetics, University of Oxford, Oxford OX3 7BN, UK. [4]Institute of Life and Health Engineering, College of Life Science and Technology, Jinan University, Guangzhou, Guangdong 510632, PR China. [5]Bayer AG Pharmaceuticals, Research & Development, Building S107, 13342 Berlin, Germany. [6]Human Genome Sequencing Center, Baylor College of Medicine, Houston, TX 77030, USA. [7]Nuffield Department of Orthopedics, Rheumatology and Musculoskeletal Sciences, University of Oxford, Botnar Research Centre, Oxford OX3 7LD, UK. [8]MRC Weatherall Institute of Molecular Medicine, University of Oxford, John Radcliffe Hospital, Oxford OX3 9DS, UK. [9]QIMR Berghofer Medical Research Institute, Brisbane, Queensland 4006, Australia. [10]Faculty of Health and Medical Sciences, University of Surrey, Guildford GU2 7YH, UK. [11]Department of Pathology, Oxford University Hospitals Foundation Trust, Oxford OX3 9DU, UK. [12]Institute for Molecular Bioscience, University of Queensland, Brisbane, Queensland 4072, Australia. [13]Division of Musculoskeletal and Dermatological Sciences, University of Manchester, Manchester M13 9PL, UK. [14]Wisconsin National Primate Research Center, University of Wisconsin-Madison, Madison, WI 53715, USA. [15]Department of Cell & Regenerative Biology and Wisconsin National Primate Research Center, University of Wisconsin-Madison, Madison, WI 53706, USA. [16]Department of Molecular and Human Genetics, Baylor College of Medicine, Houston, TX 77030, USA.
*Corresponding author. Email: thomas.tapmeier@monash.edu (T.T.T.); krina.zondervan@wrh.ox.ac.uk (K.T.Z.)
†These authors contributed equally.

RESULTS

Low-frequency coding variants in *NPSR1* are associated with familial endometriosis.

We previously demonstrated linkage of chromosome 7p13-15 with endometriosis, likely attributable to low-frequency risk variants, in an analysis of 52 families each with three or more women surgically diagnosed with the disease (*10*). Here, we conducted fine-mapping nonparametric linkage analysis and haplotype analysis of this region using 32 families that contributed to the linkage signal (see Materials and Methods) and narrowed the region of interest to a 5-Mb segment flanked by D7S683 and D7S510, centered around D7S2251. This chromosomal segment contained 28 genes (Fig. 1A).

We next sequenced this 5-Mb region in eight unrelated women from the eight families contributing most to the linkage signal. Of the 28 genes in the region, 5 harbored ≥1 nonsynonymous, predicted deleterious coding variants (see Materials and Methods) in at least 50% of the sequenced families: *EEPD1, KIAA0895, AOAH, ELMO1*, and *NPSR1*. We performed targeted sequencing of these five genes in the remaining 100 cases and 5 controls from the 32 families contributing positively to the 7p13-15 linkage signal [logarithm of odds (LOD) > 0.1] and in an additional 100 unrelated population-based controls (for details, see Materials and Methods and Supplementary Materials and Methods). We found an overrepresentation of cases with ≥1 low-frequency variants (MAF < 0.05), nonsynonymous coding variants in *NPSR1* compared to controls (Fig. 1B).

In total, three different missense variants in *NPSR1* were found in 9 of 32 families (pedigrees in fig. S1): (i) variant c7_34698148 (p.Gly42Cys, coordinates build 37), hitherto unknown, in a family

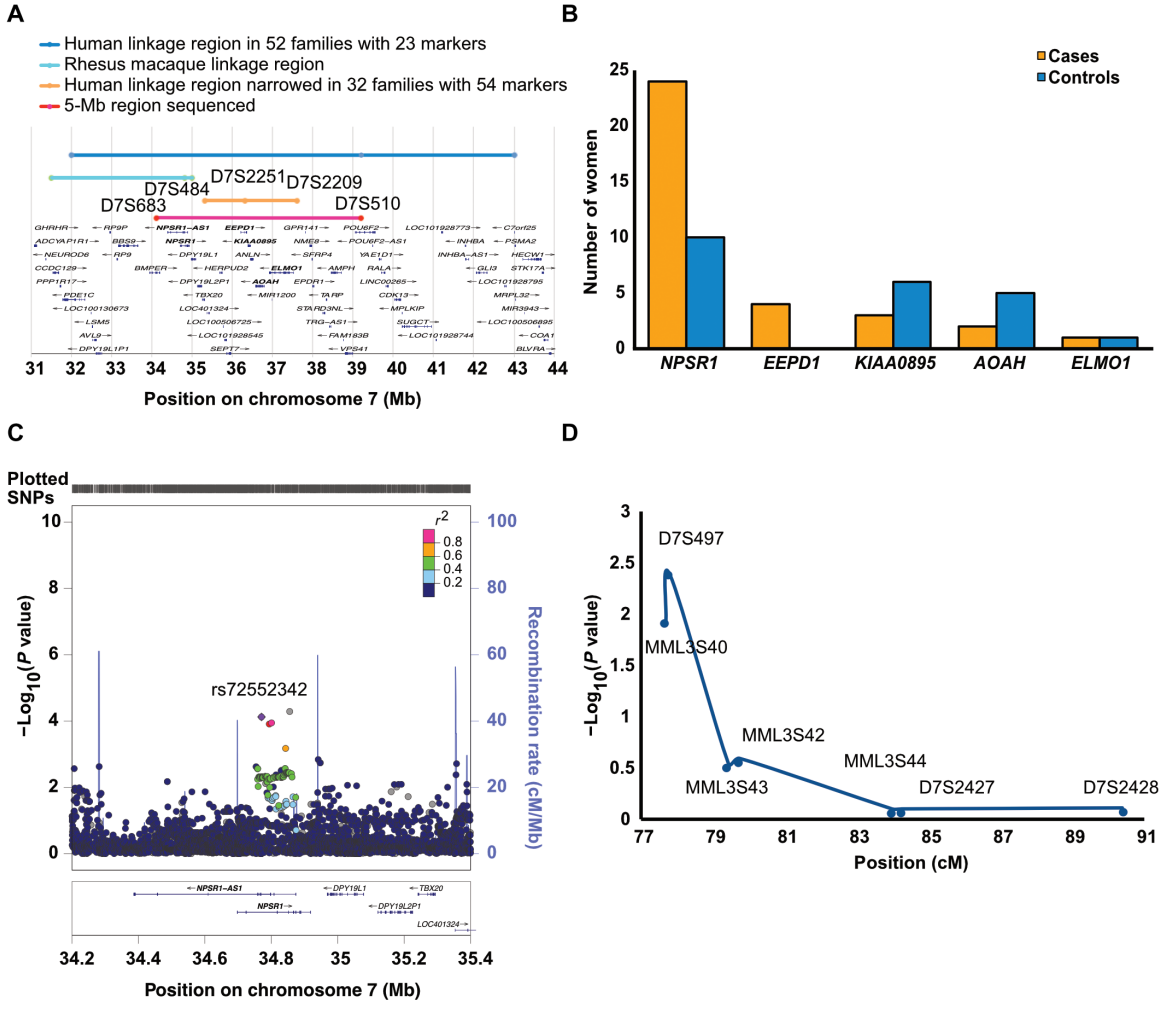

Fig. 1. Evidence for rare and common genetic variants associated with *NPSR1* from the 7p14.2 region in humans and rhesus macaque. (**A**) Physical location plot (HG build 19) of the original linkage evidence from 52 human families with three or more endometriosis cases [blue line (*10*)], additional fine-mapping linkage analysis in 32 families (yellow line), and linkage analyses in the rhesus macaque pedigree (cyan line). Each line represents the physical boundaries of endometriosis linkage regions defined by LOD-1. The 5-Mb area selected for sequencing (magenta line) is shown flanked by D7S683–D7S510, centered around D7S2251. (**B**) Number of women with noncoding, predicted deleterious, rare variants in five genes among 100 familial cases (orange) and 105 familial and population-based controls (blue). (**C**) Regional LocusZoom association plot for *NPSR1* on chromosome 7p14.2 region for stage III/IV endometriosis (1686 cases versus 7060 controls). The *y* axis shows $-\log_{10}$(*P* value) of association, and the *x* axis shows the genomic location (HG build 19). The top associated SNP is colored purple; other SNPs are colored according to the strength of linkage disequilibrium (LD) with the top SNP (r^2 in the European 1000 Genomes V3 reference dataset; the top associated indel, marked in gray, was not included given the lack of LD data on nonbiallelic variants in the 1000GV3 reference dataset). (**D**) Significant linkage of endometriosis to the region orthologous to human 7p14.2 in an extended pedigree of 849 rhesus macaques containing 135 affected animals (D7S497: $P = 0.0095$).

with five affected sisters (the family contributing most to the linkage signal), where the variant was present in all affected sisters, and (ii) two low-frequency variants, rs34705969 [1000 Genomes Phase V3 (1000GV3): MAF = 0.025, p.Cys197Phe], in four families, present in 6 of 12 genotyped cases, and (iii) rs116825950 (1000GV3: MAF = 0.025, p.Gly358Asp) in another set of four families, present in 11 of 12 genotyped cases. Not counting the hitherto unknown variant, based on the population-based MAF of the two known variants, we would have expected 3 of the 32 families to carry one of the two known single-nucleotide polymorphisms (SNPs) (Supplementary Materials and Methods), but we found 8 such families. The binomial probability of observing 8 of 32 families carrying at least one of these known variants on the basis of their population frequency is $P = 7.8 \times 10^{-4}$, a significant overrepresentation. Of the 25 cases with known ASRM disease stage in the nine families, 18 (72%) had been diagnosed with stage III/IV and 7 (38%) with stage I/II.

We subsequently genotyped all 3 missense variants implicated in familial endometriosis, as well as 20 other coding variants in *NPSR1* present on the Illumina Infinium Exome array (Supplementary Materials and Methods) in 3155 endometriosis cases and 2332 population controls from two datasets as part of a genome-wide association study (GWAS) (*11*). One of the three familial variants (rs34705969) could not be genotyped because of primer design issues, and of the remaining 22 variants, only 5 with MAF < 0.01 and 2 with MAF < 0.10 were polymorphic (table S1). Single SNP analysis of these low-frequency variants did not show significant association with overall endometriosis, nor did burden analysis of the minor allele count across SNPs with overall endometriosis ($P = 0.12$). However, aggregate analysis limited to cases with a known family history of endometriosis showed significant association ($P = 0.04$).

Common variants of *NPSR1* are associated with endometriosis

The implicated variants in *NPSR1* were low-frequency coding variants. We next investigated whether common variants mapping to/near *NPSR1* and its ligand *NPS* were also associated with endometriosis using a genome-wide association dataset of surgically confirmed cases (*11*). We analyzed all common variants (MAF > 0.01) ±500 kb of *NPSR1* from a published genome-wide association dataset of all endometriosis (3194 cases), stage I/II (1364 cases), stage III/IV (1686 cases), and familial stage III/IV (606 cases) versus 7060 controls (see Materials and Methods). Using a Bonferroni-adjusted P value threshold of $P < 5.5 \times 10^{-5}$ allowing for 903 independent tests (Supplementary Materials and Methods), we observed a significant association of rs142885915 in *NPSR1* (Indel chr7:34,855,387, MAF = 0.11) with stage III/IV endometriosis [$P = 5.15 \times 10^{-5}$; odds ratio, 1.23; 95% confidence interval (CI), 1.09 to 1.39; Fig. 1C] but not when including all endometriosis stages or stage I/II disease alone (fig. S2, A to C). Data from the Genotype-Tissue Expression (GTex) database (*12*) suggested that the deletion (G- versus GA) at rs142885915 is associated with reduced expression of NPSR1 in cerebellum ($N = 209$; normalized effect size = −0.58; $P = 6.1 \times 10^{-5}$) but with increased expression in the frontal cortex ($N = 175$; normalized effect size = 0.255; $P = 0.09$; fig. S3). Rs142885915 was not in linkage disequilibrium with the two low-frequency variants rs34705969 ($r^2 = 0.006$) and rs116825950 ($r^2 = 0.002$) found in the family-based sequencing analysis. No significant association with common variants in *NPS* was observed (fig. S2, D to F).

NPSR1 variants are present in rhesus macaques diagnosed with endometriosis

Parallel to the human studies, we conducted genetic analyses in a large multigenerational pedigree of rhesus macaques with spontaneous endometriosis, in which we had previously demonstrated familial aggregation of disease (*13*). Using both human- and rhesus macaque–specific microsatellite markers (tables S2 and S3; also see Supplementary Materials and Methods), we genotyped 418 of the 849 phenotyped animals in regions orthologous to the two significant linkage regions previously identified in humans: human chromosomes 10q26 (*14*) and 7p13-15 (*10*). We conducted simulation-based nonparametric linkage analysis obtaining empirical significance estimates to allow for the complex pedigree structure (see Materials and Methods). Although no significant linkage was found on the macaque ortholog of human chromosome 10 (minimum $P = 0.5$; fig. S4), we found significant linkage between D7S497 located on rhesus macaque chromosome 3 (ortholog of human chromosome 7) and endometriosis [minimum $P = 0.0095$ (D7S497); Fig. 1D].

Given the strong signal in *NPSR1* under the human linkage peak, we conducted targeted sequencing of *NPSR1* in 62 rhesus macaque cases and 49 controls (table S4). We identified 10 missense variants. Three rare missense variants were seen at MAF < 0.05 in cases and were not observed in controls. Three additional missense variants were more prevalent in cases than in controls. In aggregate, 44 of 544 (8.09%) of alleles in rhesus macaque cases carried at least one of the six missense variants exclusive to or prevalent in the cases compared with 26 of 512 (5.08%) alleles in rhesus macaque controls. The sample size was insufficient to warrant statistical testing for genetic association with disease after adjusting for familial relationships. These parallel genetic analyses in two species suggested a role for *NPSR1* in the pathogenesis of endometriosis.

NPSR1 is expressed in endometrial tissues and on monocytes in peritoneal fluid

Given the probable role of endometrial biochemistry and pathophysiology as well as immune response in endometriosis pathogenesis (*1*), we tested for the presence of NPSR1 and its cognate ligand NPS in endometrial tissue, as well as on immune cells present in peritoneal fluid (PF). Eutopic endometrial tissue and endometriotic (ectopic) tissue sections from 13 patients with endometriosis at different ASRM disease stages and at different stages of the menstrual cycle, and eutopic endometrium from seven controls with no evidence of endometriosis were stained with anti-NPSR1 and anti-NPS antibodies (Fig. 2A; fig. S5; isotype stainings, fig. S6). NPSR1 was strongly expressed in glandular epithelial cells in both eutopic and ectopic endometrium, showing darkly stained nuclei surrounded by lighter-stained cellular membranes. Conversely, NPS was expressed in the stroma but not in the glandular epithelium, whereas NPSR1 staining was sparse in the stroma. We did not find a perivascular expression pattern of either NPSR1 or NPS (fig. S7). This suggests a paracrine signaling mechanism within the organ with ligand and receptor in close proximity, similar to what has been observed in the lung (*15*) and the gastrointestinal tract (*16*).

We measured the expression of *NPSR1* in 49 samples by quantitative reverse transcription polymerase chain reaction (qRT-PCR) (Fig. 2B) and found that amounts were similar in eutopic endometrium from patients with endometriosis and unaffected controls, as well as in endometriotic tissue [$n = 11$ to 26 per group; $P = 0.20$, analysis of variance (ANOVA) with Dunnett's multiple comparisons test];

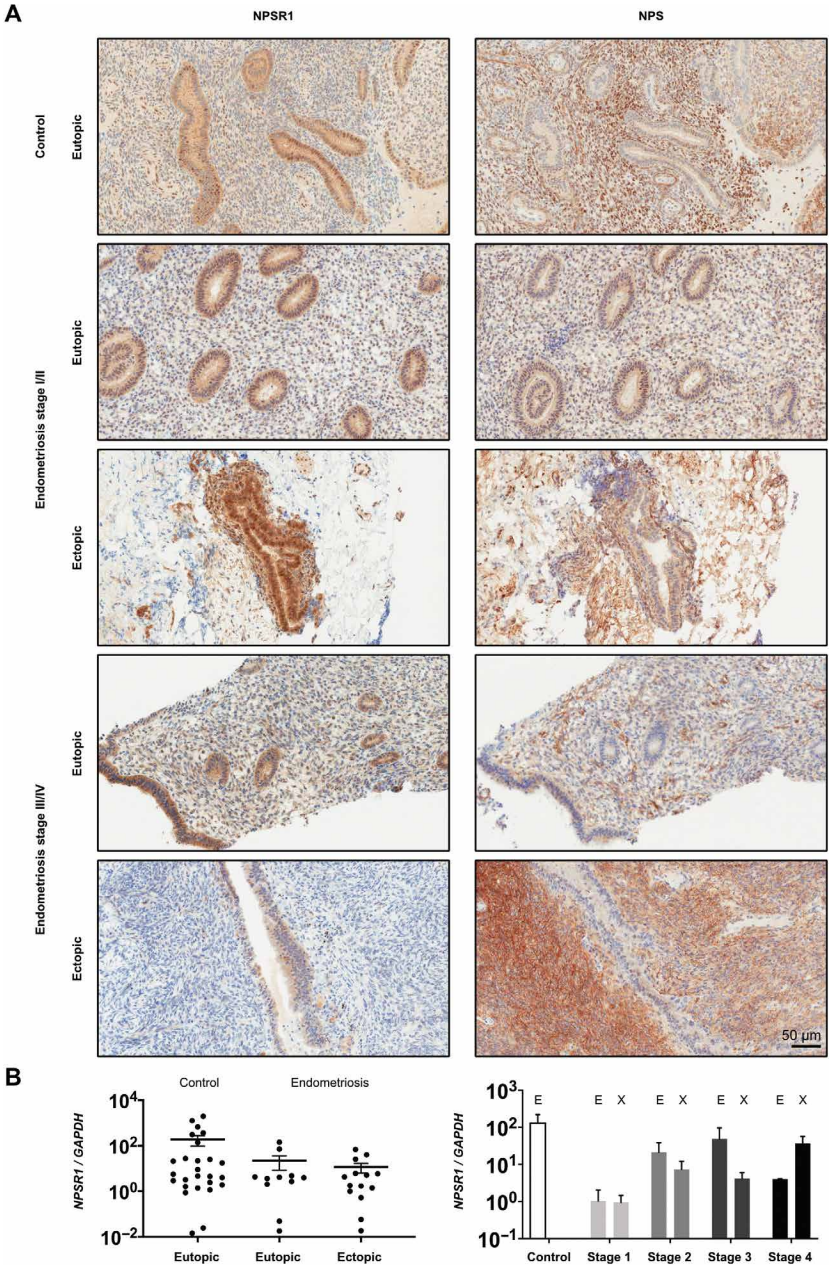

Fig. 2. NPSR1 and its ligand NPS are expressed in the endometrium. (**A**) Tissue samples of proliferative phase endometrium from patients with minimal/mild (stages I/II) or moderate/severe (stages III/IV) endometriosis were stained with anti-NPSR1 and anti-NPS antibodies, respectively (DAB, brown color). Endometrium from disease-free controls was stained along with the patient samples. (Magnification ×200; scale bar, 50 μm; representative images shown.) (**B**) qRT-PCR was done on eutopic and ectopic endometrium from patients and nonendometriotic controls. The expression of *NPSR1* was normalized to *GAPDH* using the $2^{-\Delta\Delta Ct}$ method and tested adjusted for cycle phase (E, eutopic; X, ectopic tissue). See fig. S6 for staining of secretory phase endometrium.

expression did not depend on ASRM stage or cycle phase (n = 2 to 5 per group; P = 0.22, Kruskal-Wallis test, with Dunn's multiple comparisons test).

We next investigated whether immune cells in PF expressed NPSR1, as previously reported for alveolar macrophages in asthmatic lungs (*17*), and whether expression levels corresponded to levels of NPS secreted into the PF (Fig. 3). Flow cytometric analysis of PF cells showed that most of the hematopoietic cells ($CD45^+$) expressed NPSR1 on their surface, with no appreciable difference in receptor expression between patients and controls (Fig. 3A; gating in fig. S8). However, in analyses stratified on menstrual cycle phase, NPS amounts were significantly increased in the PF of patients versus controls during the luteal phase and menstruation but not during the proliferative phase (P = 0.013 during luteal phase; P = 0.024 during menstruation; 70 patients versus 38 controls, Mann-Whitney U test; Fig. 3B). We tested for association of the amount of NPS in PF, accounting for menstrual cycle phase: NPS amount was associated with disease status (P = 0.0472; logistic regression adjusting for cycle phase, NPS levels as predictor and endometriosis status as outcome) but not with cycle phase (P = 0.7). We used mass cytometry by time of flight (CyTOF) to discriminate between the $NPSR1^+$ leukocyte populations of the PF and identified a population of infiltrating monocytes highly positive for NPSR1 in patients but not in controls (Fig. 3C and tables S5 and S6). No differences in NPSR1 expression by menstrual cycle phase were observed (fig. S9).

Inhibition of NPSR1 abrogates proinflammatory signaling in monocytes in vitro

Monocytes have previously been described as expressing NPSR1 (*17*), which signals upon binding of NPS through the $G\alpha_q$ and $G\alpha_s$ subunits of the G protein coupled to the receptor and subsequently through Ca^{2+} mobilization and cyclic adenosine monophosphate (cAMP) signaling, respectively (Fig. 4A) (*18*). Downstream effects of NPS signaling include tumor necrosis factor–α (TNF-α) release (*19*) and chemotactic behavior toward NPS (*20*).

We used the small molecular inhibitor SHA 68 (3-oxo-1,1-diphenyl-tetrahydro-oxazolo[3,4-a]pyrazine-7-carboxylic acid 4-fluoro-benzylamide) (Fig. 4B) (*21*) to inhibit NPSR1 signaling in monocytes and evaluated the inhibitory effect on different stages of NPS/NPSR1 signal transduction in vitro, including receptor dimerization, subsequent release of Ca^{2+} and cAMP second messengers, and TNF-α release, and on chemotaxis of human monocytes from healthy controls toward NPS. After confirming the R enantiomer as the inhibitory isomer (Fig. 4C), we used SHA 68R in all subsequent experiments.

The inhibitor showed a dose-dependent inhibition of NPSR1 receptor activation as determined by reduced β-arrestin binding (Fig. 4D), demonstrating a median effective concentration (EC_{50}) for NPS of 88 nM (pEC_{50} = 7.06) and a median inhibitory concentration (IC_{50}) of 86 nM [pK_a (where K_a is the acid dissociation constant) = 7.07], confirming previous studies (*22*, *23*). We found both cAMP and Ca^{2+} signaling inhibited by SHA 68R in a dose-dependent fashion (Fig. 4, E to G). In the cAMP assay, the EC_{50} of NPS was 90 nM (pEC_{50} = 7.04), and the IC_{50} of the inhibitor SHA 68R was 15.3 nM (pK_a = 7.8), also as expected (*21*). Ca^{2+} signaling was quantified via increase in fluorescence of calcium-bound Fura

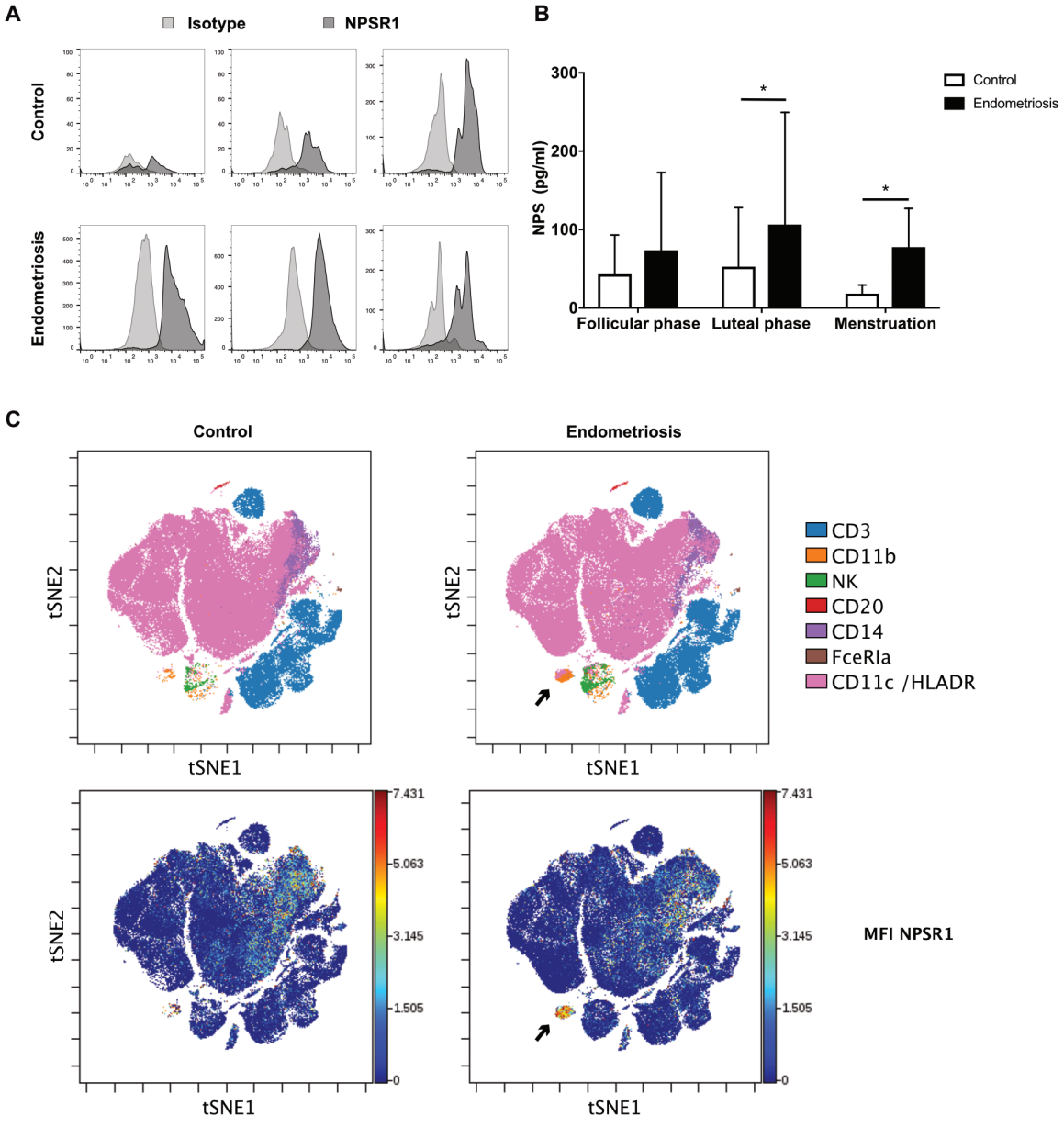

Fig. 3. NPS is elevated and NPSR1 is prominently expressed on monocytes in PF from patients with endometriosis. (**A**) Hematopoietic CD45$^+$ cells from PF of patients with endometriosis and nonendometriotic controls were stained with anti-NPSR1 (dark shaded peak) versus isotype controls (light) and measured by flow cytometry. NPSR1 is widely expressed on hematopoietic cells within PF in both controls and endometriosis ($n = 3$ per group). (**B**) The amount of NPS in the PF of patients and controls was measured by ELISA. Samples were grouped by menstrual cycle phases to account for variations caused by follicular phase ($n = 15$, control and $n = 28$, endometriosis), luteal phase ($n = 19$, control and $n = 32$, endometriosis; $P = 0.013$, Mann-Whitney U test), and menstruation ($n = 4$, control and $n = 10$, endometriosis; $P = 0.024$, Mann-Whitney U test). (**C**) PF of 20 patients and 20 controls was analyzed using cytometry by time of flight (CyTOF) and a panel of leukocyte markers (table S5). The analysis of samples concatenated by group using the visual stochastic neighbor embedding (viSNE) algorithm reveals a cell population highly positive for NPSR1 within patients with endometriosis but not in controls. Back-gating of the population shows the NPSR1$^+$ cells to be CD11b$^+$ inflammatory monocytes (arrows).

Red dye (*24*), with the peak produced proportional to the NPS dose given (Fig. 4F and fig. S10). We observed an inhibition of NPS-induced Ca^{2+} mobilization by 0.16 μM SHA 68R on primary human monocytes ($P = 0.0187$, ANOVA with Dunnett's multiple comparisons test against NPS 100 nM).

One of the hallmarks of endometriosis is a chronic inflammation in the peritoneum, with prominent involvement of cytokines such as TNF-α. We therefore tested the ability of SHA 68R to inhibit TNF-α release after lipopolysaccharide (LPS) and NPS stimulation of monocytic THP-1 cells and found that SHA 68R decreased the amount of TNF-α significantly at a dose of 10 nM ($P = 0.0140$, ANOVA with Dunnett's multiple comparisons test against SHA 68R 0 nM; Fig. 4H).

Last, we tested the effects of SHA 68R on NPS-mediated monocyte chemotaxis to determine the dose to be used to inhibit monocyte infiltration in vivo (Fig. 4I). We used 100 nM NPS to induce chemotaxis

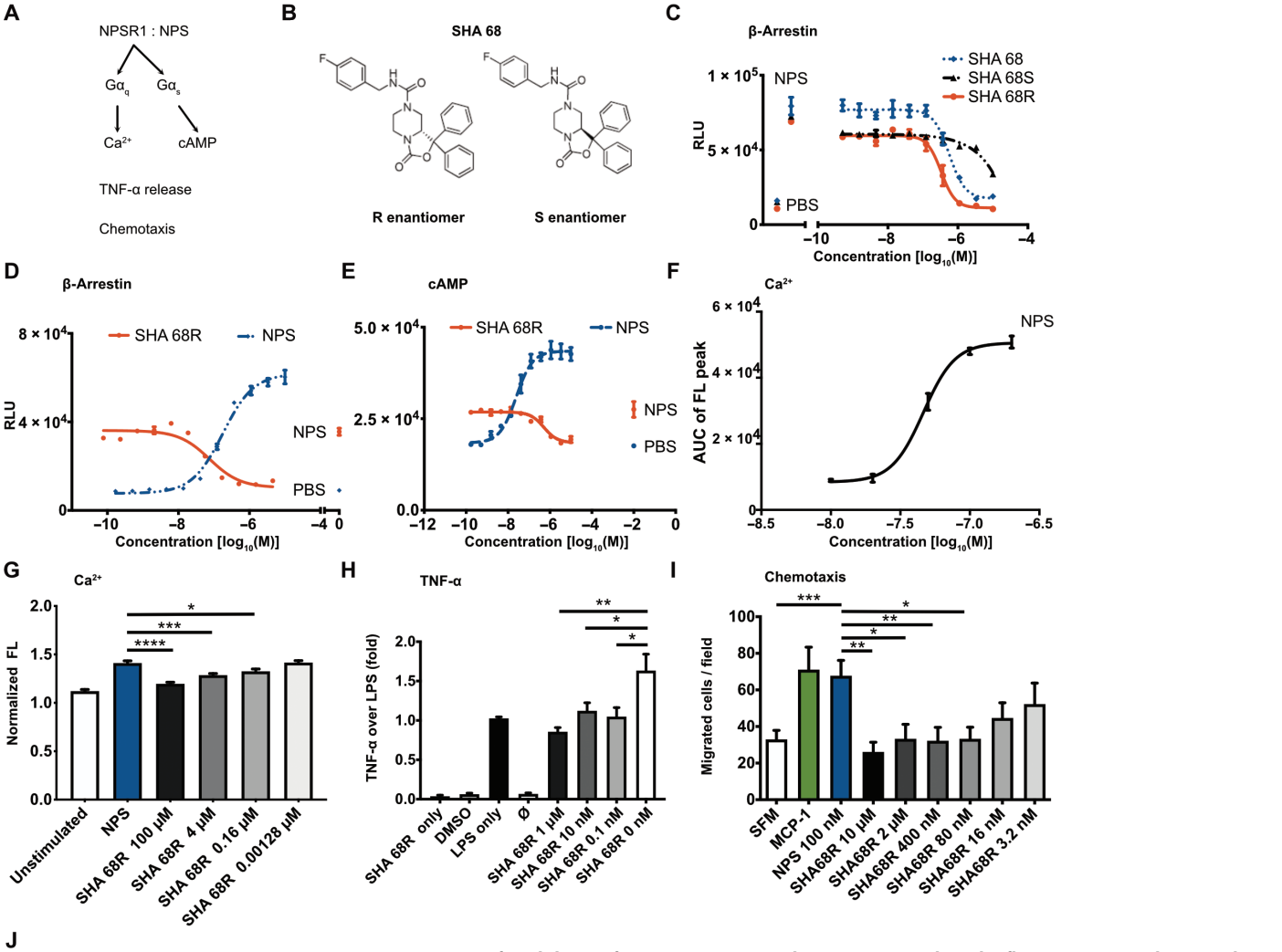

Fig. 4. A specific inhibitor of NPSR1, SHA 68R, reduces NPSR1-mediated inflammatory signaling in a dose-dependent manner. (**A**) Upon binding of its ligand NPS, NPSR1 signals downstream through the G protein subunits $G\alpha_q$ and $G\alpha_s$, with intracellular calcium (Ca^{2+}) and cAMP (*18*, *53*). Downstream effects are TNF-α release (*16*) and chemotaxis (*20*). (**B**) Structure of the R and S enantiomers of SHA 68 (*52*). (**C**) The inhibitory effect on NPSR1 signaling of the racemic mixture and the R and S enantiomers were tested in the β-arrestin assay ($n = 2$ wells per dose). (**D**) The IC_{50} of SHA 68R against NPS activation of NPSR1 was determined as 86.4 nM in the β-arrestin assay (NPS, 100 nM; $n = 4$ wells per dose, seven technical replicates). (**E**) Dose-dependent inhibition of cAMP signaling; IC_{50}, 0.5 µM (NPS, 100 nM; $n = 2$ wells per dose). (**F**) Dose response curve of primary human monocytes loaded with Fura dye to indicate the intracellular release of calcium ions (Ca^{2+}) and stimulated with increasing doses of NPS. The release of Ca^{2+} ions led to a peak in fluorescence (see fig. S6); the area under curve (AUC) was quantified as an indicator of signaling strength. NPS induction of intracellular Ca^{2+} release, $EC_{50} = 46.32$ nM ($n = 8$ wells per dose). (**G**) Primary human monocytes were preincubated with SHA 68R for 30 min and used in the Fura Red Ca^{2+} assay (*$P = 0.0187$; ***$P = 0.0002$; ****$P < 0.0001$; $n = 2$ to 14 per dose, four biological replicates; ANOVA with Dunnett's multiple comparisons test against NPS 100 nM). (**H**) THP-1 cells were preincubated with SHA 68R for 30 min at the doses indicated. Cells were stimulated with LPS and NPS, or with LPS alone. The amount of TNF-α released after 6 hours was measured by ELISA ($n = 6$ per dose, three biological replicates, SHA 68R 1 µM, **$P = 0.0013$; SHA 68R 10 nM, *$P = 0.0331$; SHA 68R 0.1 nM, *$P = 0.0140$; ANOVA with Dunnett's multiple comparisons test against SHA 68R 0 nM). (**I**) Primary human monocytes were preincubated for 30 min with the indicated dose of SHA 68R and used in a chemotaxis assay against NPS over 2 hours [$n = 4$ to 6 wells per dose, six biological replicates; ***$P < 0.001$, unpaired t test, serum-free medium (SFM) versus NPS 100 nM; *$P < 0.05$, **$P < 0.01$, ANOVA with Dunnett's post-test against NPS 100 nM; ANOVA with analysis for trend within SHA 68R treatment groups, $P = 0.0017$; IC_{50}, 28.31 nM]. (**J**) Exposure testing of SHA 68R for in vivo experiments. C57BL/6 mice ($n = 3$ per group) were injected intraperitoneally (i.p.) or subcutaneously (s.c.) with the inhibitor SHA 68R (40 mg/kg), and blood samples were taken at intervals to determine the amount of unbound SHA 68R in circulation. Data are presented as means ± SEM.

in human monocytes and determined an IC_{50} of 28 nM for SHA 68R ($pK_a = 7.55$) against NPS-induced chemotaxis.

We then tested the pharmacokinetics of SHA 68R in C57BL/6 mice to determine whether an appropriate dose could be given to maintain unbound inhibitor over the time frame needed for in vivo experiments and whether an intraperitoneal or subcutaneous injection would be favorable (Fig. 4J). We found that an injection of SHA 68R (40 mg/kg, subcutaneously) delivered sufficient amounts to inhibit monocyte chemotaxis (28 nM) for up to 4 hours without any side effects in behavior or appearance.

Inhibition of NPSR1 reduces pain and inflammation in peritonitis and endometriosis mouse models

Last, we investigated the effect of NPSR1 inhibition in vivo in inflammatory models used in endometriosis research (Fig. 5 and figs. S11 and S12). We used the zymosan-induced peritonitis (ZIP) model, which shares many characteristics with human peritoneal inflammation, most importantly the influx of F4/80^{low} 7/4^{+} monocytes and increased cytokine levels (*25*), in C57BL/6 mice. We measured the number of infiltrating monocytes in comparison to the F4/80^{+} 7/4^{-} resident macrophages (Fig. 5, A and B, and fig. S11) and found SHA 68R effective in reducing the number of infiltrating monocytes at a dose of 40 mg/kg (n = 9 to 12 mice per group; $^{**}P$ = 0.0011, ANOVA; $^{**}P$ = 0.0096, test for linear trend, 0, 10, and 40 mg/kg of SHA 68R; Fig. 5B). Blood plasma concentrations of the inflammatory cytokines interleukin-4 (IL-4), IL-12p40, and IL-17 were significantly reduced (n = 8 to 10 mice per group; IL-4 $^{*}P$ = 0.0413, IL-12p40 $^{**}P$ = 0.0010, and IL-17 $^{*}P$ = 0.0409, 40 mg/kg versus control; Fig. 5C). Because not all mice produced data points within the detection limit, a two-way ANOVA could not be performed and we used a mixed-effects model analysis instead, with Holm-Sidak correction for multiple comparisons. We confirmed the anti-inflammatory effect of SHA 68R in an experimental model of endometriosis in BALB/c mice, involving the inoculation of 12 uterine tissue fragments derived from syngeneic estrous phase-matched donor BALB/c mice into the peritoneal cavity. The amounts of inflammatory cytokines were decreased by SHA 68R (n = 8 to 11 mice per group; IL-1b $^{*}P$ = 0.0228 and IL-12p40 $^{*}P$ = 0.0178; Fig. 5D and fig. S11). To measure the effect of NPSR1 inhibition on abdominal pain as the main symptom of endometriosis, we used the dynamic weight bearing (DWB) assay (Fig. 5, E and F) (*26*) and found SHA 68R effective in reducing abdominal pain–related spontaneous behaviors in both the ZIP (n = 10 mice per group; P = 0.0315, unpaired t test; 40 mg/kg SHA 68R versus control) and endometriosis inoculation models (n = 8 mice per group; P = 0.0263, unpaired t test; 40 mg/kg SHA 68R versus control). In line with previous studies, the induction of pain-associated behavior became apparent in the control groups during day 2 (Fig. 5F), with SHA 68R significantly reducing pain-associated behavior at the time of the therapeutic window.

DISCUSSION

Endometriosis represents an unmet clinical need (*1*), with annual direct health care costs similar to those of type 2 diabetes. Treatment of endometriosis is limited to surgical removal of endometriotic

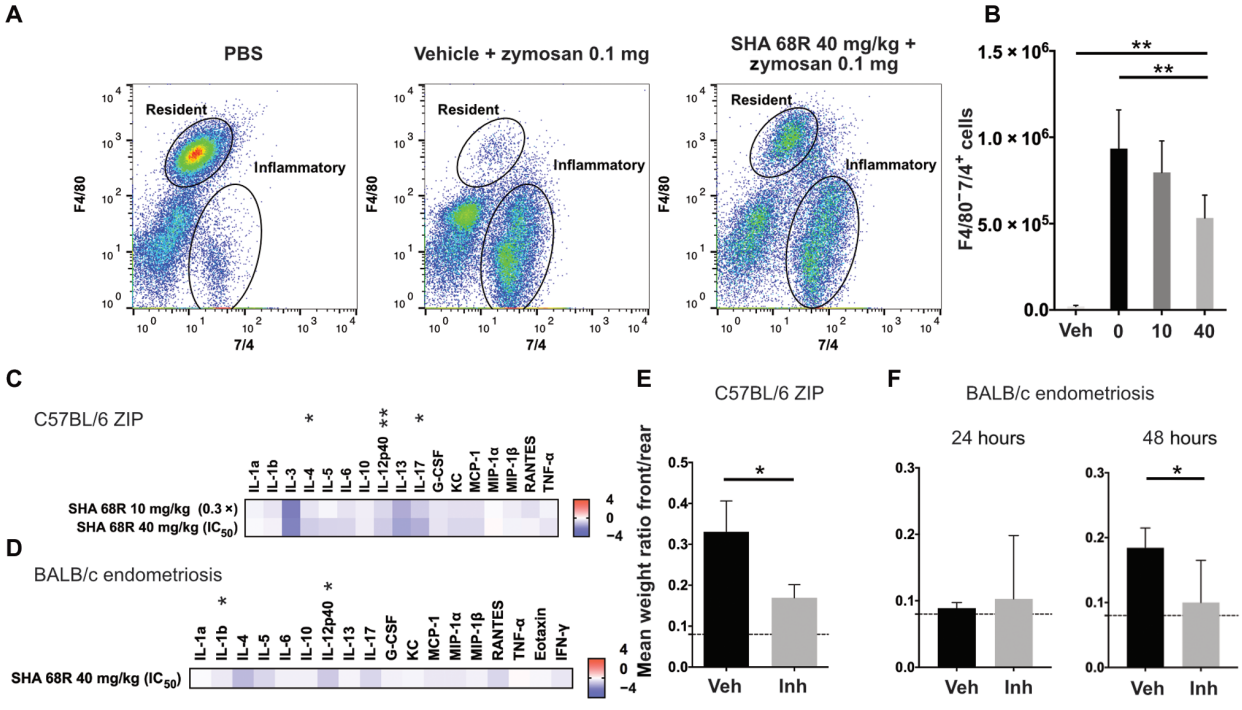

Fig. 5. The inhibition of NPSR1 reduces peritoneal inflammation and abdominal pain in vivo. The efficacy of NPSR1 inhibition in vivo was tested in mouse models. (**A**) C57BL/6 mice were injected subcutaneously with SHA 68R or vehicle 1 hour before zymosan was injected intraperitoneally to induce inflammation. An injection with PBS instead of zymosan was done to document the baseline distribution of cells within the peritoneum. Four hours after zymosan injection, the mice were sacrificed and the peritoneal exudate was harvested. Cells were analyzed by flow cytometry using markers for resident macrophages (F4/80) versus infiltrating monocytes (7/4). Plots shown are representative (n = 9 to 12 mice per group). (**B**) Quantification of the F4/80^{-}7/4^{+} inflammatory monocytes in the peritoneum (doses in mg/kg; n = 9 to 12 mice per group, $^{**}P$ = 0.0011, ANOVA; $^{**}P$ = 0.0096, test for linear trend, 0, 10, and 40 mg/kg SHA 68R). (**C**) Plasma cytokines were measured in the ZIP model (n = 8 to 10 mice per group; data normalized to vehicle-only treatment, $\log_2$ up-/down-regulation; IL-4 $^{*}P$ = 0.0413, IL-12p40 $^{**}P$ = 0.0010, IL-17 $^{*}P$ = 0.0409, 40 mg/kg versus control, mixed-effects model analysis with Holm-Sidak correction for multiple comparisons). (**D**) SHA 68R (40 mg/kg) was used in the endometriosis model in BALB/c mice (n = 8 to 11 mice per group; data normalized to vehicle-only treatment, $\log_2$ up-/down-regulation; IL-1b $^{*}P$ = 0.0228, IL-12p40 $^{*}P$ = 0.0178, mixed-effects model analysis with Holm-Sidak correction for multiple comparisons). (**E**) The ratio of weight borne on the front versus rear paws was measured as an indicator of abdominal pain 4 hours after zymosan challenge and SHA 68R treatment (Veh, vehicle; Inh, 40 mg/kg SHA 68R, subcutaneously). The dashed line indicates the situation in PBS-injected mice (n = 10 mice per group; $^{*}P$ = 0.0315, unpaired t test). (**F**) In the BALB/c endometriosis model, dynamic weight shifting was recorded 24 and 48 hours after inoculation when pain manifests in this model (n = 8 to 10 mice per group; $^{*}P$ = 0.0263, unpaired t test).

tissue or hormonal medication mainly aimed at estrogen suppression. Alternative treatments with fewer side effects are urgently required. Despite genetic studies suggesting that the pathogenesis of ASRM stage I/II disease is genetically distinct from stage III/IV (*27*), no treatments targeted toward specific disease subtypes have been developed.

Our study combined evidence from genetic analyses of endometriosis in humans and rhesus macaques to identify a nonhormonal target for therapeutic intervention: the G protein–coupled cell surface receptor NPSR1. Naturally occurring primate genetic models of human disease have been described for human single-gene disorders (*28*, *29*), but to our knowledge, this is the first example of parallel investigations in which both human and nonhuman primate data were used together to identify a genetically validated therapeutic target. Following our previously reported linkage signal for endometriosis on chromosome 7p13-15 (*10*), we used fine-mapping, haplotyping, and next-generation sequencing approaches in families contributing to the linkage signal and additional linkage and sequencing analysis in rhesus macaques with spontaneous disease. These analyses uncovered an association of low-frequency, missense coding variants in *NPSR1* with familial, predominantly ASRM stage III/IV, endometriosis. Targeted analyses of large-scale GWAS data for surgically confirmed cases (*11*) also highlighted the association of common noncoding *NPSR1* variants with stage III/IV endometriosis in the general population.

Genetic variants in *NPSR1* have been associated with a range of inflammatory and neuropsychiatric phenotypes, including asthma (*30*, *31*), allergy (*32*, *33*), inflammatory bowel disease (IBD) (*16*, *34*), rheumatoid arthritis (*35*), panic disorders (*36*), psychological stress (*37*), fear responses (*38*), and recurrent abdominal pain (*39*). The common insertion/deletion variant associated with endometriosis in *NPSR1*, rs142885915, is intronic, has a frequency of 11.3% in European ancestry populations, and is independent from common variants previously associated with IBD, asthma, and neuropsychiatric phenotypes (linkage disequilibrium between variants $r^2 < 0.1$). GTex data suggest that the effects of the deletion are likely tissue dependent, with evidence for associated down-regulation of NPSR1 in cerebellum and up-regulation in the frontal cortex. Intriguingly, independent variants in *NPSR1* associated with abdominal pain, rs2530566G (*39*), and IBD, rs2530547 (*40*), show the exact same pattern in GTex (accessed January 2021) of association with NPSR1 expression. Both brain areas—but the frontal cortex in particular—are activated in pain perception (*41*). The tissue-specific effects of this deletion after sustained inflammatory insult as in endometriosis require further functional work. One of the low-frequency missense mutations observed to be associated with familial endometriosis, rs34705969 (p.Cys197Phe), has been described as resulting in a reduced ability to induce downstream gene expression changes or cAMP-mediated signaling (*40*). The effects of the other two missense variants rs116825950 (p.Gly358Asp) and the hitherto unknown variant C7_34698148 (p.Gly42Cys) on NPSR1 structure or function are unknown. The genetic validation of the potential role of NPSR1 in endometriosis is important because it greatly increases the likelihood for a drug target modulator to be approved for clinical use (*42*).

NPS is encoded on chromosome 10p26.2, the second linkage area reported for endometriosis (*14*). Future studies may benefit from investigating the role of rare NPS variants on the cell-specific function of NPS in endometriosis. Following our genetic analyses, we demonstrated functional effects of *NPSR1* on proinflammatory processes in both in vitro and in vivo experiments. We identified a population of infiltrating monocytes highly positive for NPSR1 in women with endometriosis and showed that inhibition of NPSR1 through a selective inhibitor, SHA 68R, resulted in reduced migration of NPS-induced monocytes in vitro. We further demonstrated an anti-inflammatory effect and a reduction of abdominal pain–induced behavior after SHA 68R administration in mice, in both a ZIP mouse model (*25*) and an inoculation model of endometriosis (*43*), with concomitant reduction in the number of infiltrating monocytes and decreased blood cytokine concentrations. The ZIP model features all stages of inflammation including the resolution phase, allowing for the study of different immune cell types involved at different stages, whereas the endometriosis model includes the presence of endometrial adhesions within the peritoneal cavity, thus mimicking the presence of lesions.

The chronic inflammatory phenotype associated with endometriosis is likely maintained by immune cells in PF (*1*). Inflammation and pain are thought to be triggered by the deposition of endometrial cellular material within the peritoneum (*5*), although the pain mechanisms can be of inflammatory and neuropathic nature (*1*). Pivotal to pathology is an aberrant wound-healing response to cellular debris (*44*). The increased levels of NPS in patients with endometriosis during the secretory and menstrual phases could augment this aberrant response by increasing monocyte recruitment.

NPSR1 expression on inflammatory cells, typically induced by inflammatory cytokines such as TNF-α and interferon-γ (*16*), is up-regulated during inflammation in asthma (*30*) and IBD (*34*). Macrophages isolated from mice in asthma models expressed NPSR1 after antigen challenge (*45*), and stimulation of these macrophages with NPS led to proinflammatory M1 polarization and increased migration. The NPS/NPSR1 system, in turn, up-regulated IL-8, one of the most prominent monocyte attractants and proinflammatory cytokines (*46*) and key in endometriosis inflammatory pathophysiology (*1*). Thus, NPS-induced signaling through NPSR1 could induce chronic inflammation, with a perpetuated feedback loop through IL-8–dependent recruitment of inflammatory monocytes, TNF-α–induced up-regulation of NPSR1, and further production of TNF-α by the new arrivals. This raises the prospect of targeting NPSR1 to interrupt the developing chronic inflammation in endometriosis and alleviate pain as its main symptom. We have shown in animal models that NPSR1 inhibition holds promise toward this goal.

We acknowledge that our study has some limitations. In endometriosis, we address a complex condition of unknown etiology. Some of our investigations did not allow for more detailed analyses, which would have been desirable. Our in vitro studies included a relatively small number of patients and did not include investigations of the functional effects of the *NPSR1* variants we identified as associated with endometriosis. Second, we focused on the inflammatory effects related to NPSR1/NPS and did not investigate its anxiety-related effects, which might have additional bearing on the experience of endometriosis-related pain symptoms. A final point is that although mouse models mimic elements of the endometriosis disease process, they cannot feature the full disease spectrum, in particular, the pathological nuances related to disease stages seen in women. Further exploration of the effect of NPSR1/NPS inhibition on endometriosis-related inflammation and pain symptoms in the rhesus macaque is desirable.

In summary, endometriosis is a common condition for which better treatment options are urgently needed. Our results suggest the NPSR1/NPS system as a genetically validated, nonhormonal target for the treatment of endometriosis, with likely increased relevance to stage III/IV endometriosis therapeutics.

MATERIALS AND METHODS

Detailed methods are available in Supplementary Materials and Methods.

Study design

The aim of this study was to (i) identify genetic target(s) from families with multiple cases of endometriosis and (ii) explore the role of the candidate gene derived from these analyses, NPSR1, as a nonhormonal treatment target for the disease. Fine-mapping linkage, haplotype, and sequencing analyses were conducted using 52 families with three or more women with endometriosis from the United Kingdom and Australia, and a large pedigree of 849 rhesus macaques with spontaneous disease. No selection of families or animals within the pedigree was applied, and all available genotype data were used. For subsequent in vitro NPSR1/NPS description and validation experiments, we used tissue and PF samples collected according to World Endometriosis Research Foundation (WERF) Endometriosis Phenome and Biobanking Harmonisation Project (EPHect) standardized protocols (*47*). We tested inhibition of NPSR1 signaling in monocytes from cases and healthy controls under identical experimental conditions, and in vivo inhibition of inflammation and pain read-outs in a peritonitis mouse model (*25*) and a mouse model of endometriosis (*26*). Sample sizes were not predetermined through statistical methods. The investigators were not blinded to the experimental conditions during experiments and the analyses.

Fine-mapping of the 7p13-15 linkage region in humans

We previously identified the linkage to chromosome 7 (D7S493-D7S502) using 23 polymorphic markers based on 52 families with three or more affected women from the OXEGENE Study (ethics approval: MREC/99/5/11) (*10*). We genotyped an additional 31 markers (table S2) across the linkage region in the 32 families contributing positively to the linkage signal (LOD > 0.1). Linkage analyses and maximum likelihood haplotype construction were conducted using Merlin (*48*).

Linkage analysis in rhesus macaques

Fourteen microsatellite markers (table S3) across two regions orthologous to the human regions previously exhibiting linkage in human families [7p13-15 and 10q26 (*10*)] were genotyped (seven markers per region) in 418 rhesus macaques from a pedigree at the Wisconsin National Primate Research Center, including 135 females with spontaneous endometriosis (*13*). Simulation-based nonparametric linkage analyses were performed using SimWalk2 (*49*).

Sequencing in humans and rhesus macaques

A 5-Mb genomic fragment centered on D7S2251 (Fig. 1A) was sequenced in eight unrelated affected women from the eight families contributing most to the 7p13-15 linkage signal. A custom NimbleGen array was used to capture the region of interest, followed by Roche 454 GS-FLX next-generation sequencing. Five of 28 genes were prioritized for further analysis because they harbored ≥1 nonsynonymous, low-frequency coding variant in ≥50% of sequenced women. The five genes were sequenced (paired-end) on Illumina HiSeq following custom NimbleGen capture in 100 remaining cases and 5 controls from the 32 families and 100 unrelated controls (see Supplementary Materials and Methods) (*10*). Sanger sequencing was used to analyze the rhesus macaque region orthologous to human *NPSR1* in 62 affected animals and 49 unaffected controls with sufficient quality DNA (table S4; see also Supplementary Materials and Methods).

Tissue and PF samples

Eutopic and ectopic endometrium as well as PF were collected from women recruited in the ENDOX Study (*50*) (REC reference 09/H0604/58, South Central—Oxford B Research Ethics Committee) according to WERF EPHect standardized protocols (*47*).

Immunohistochemistry

Samples were collected in ice-cold phosphate-buffered saline (PBS), fixed in paraformaldehyde (4%, 1 hour) and ethanol (100%, overnight), and embedded in paraffin blocks. Serial sections (5 μm) were used for hematoxylin and eosin (H&E) and antigen-specific staining. Antibodies used were anti-NPSR1 (1:1500), anti-NPS (1:1000) (Abcam), and an anti-rabbit secondary antibody, and 3,3′-diaminobenzidine (DAB) was used for visualization with hematoxylin counterstaining.

Quantitative reverse transcription polymerase chain reaction

RNA was extracted from snap-frozen tissue samples, and 1 μg of RNA per sample was reversely transcribed. Complementary DNA (cDNA) (100 ng) was used in an SYBR Green real-time PCR assay. Primers and conditions were as published previously (*40*), with a melting curve run to ascertain specific amplification. Relative expression of *NPSR1* versus *GAPDH* was calculated using the $\Delta\Delta C_t$ method (*51*).

Flow cytometry

Pure PF samples were washed and stained (Supplementary Materials and Methods) and incubated with anti-NPSR1–AF488 (polyclonal rabbit) or an isotype control (both Bioss Inc.) and anti-CD45 BV605 (BD Biosciences) at a 1:320 dilution for 1 hour on ice in the dark. Cells were washed twice in PBS/bovine serum albumin (1%), resuspended in 100 μl, and measured in a Fortessa flow cytometer (Beckton Dickinson).

Cytometry by time of flight

Purified antibodies (table S5) were labeled with metal tags using Maxpar Antibody Labeling Kits (DVS Sciences) as per the manufacturer's instructions. Labeled antibodies were titrated to determine the working concentration. Details of the patient samples used for CyTOF analysis are given in table S6.

Enzyme-linked immunosorbent assay

NPS in PF supernatants was measured by enzyme-linked immunosorbent assay (ELISA) (CEA796Hu, Cloud Clone Corp.) according to the manufacturer's instructions.

SHA 68R

The inhibitor compound was synthesized as previously described (*52*).

Monocytes

Primary human monocytes were isolated from blood samples from healthy donors using Ficoll-Paque PLUS/Percoll (GE Healthcare

Life Sciences) centrifugation according to the manufacturer's instructions (detailed method in Supplementary Materials and Methods).

Mouse experiments

All experiments were performed at Bayer AG in accordance with local policies and directives (Landesamt für Gesundheit und Soziales Berlin, Germany) and at Oxford in accordance with the Animals (Scientific Procedures) Act 1986 Amendment Regulations 2012 (ASPA 2012), UK.

ZIP model

The ZIP model was performed as previously described (*25*). Female C57BL/6 mice (8 to 12 weeks old) were injected subcutaneously with SHA 68R (40 mg/kg in cyclodextrin, 10%, 50 μl) or vehicle. One hour later, zymosan was administered (0.1 mg in 200 μl of PBS, intraperitoneally). Four hours after zymosan administration, tail vein blood samples were collected under terminal anesthesia and the mice were sacrificed, the abdominal skin was opened, and the peritoneum was washed with 3 ml of ice-cold PBS with 5 mM EDTA to obtain peritoneal exudate cells (PECs). PECs were counted and stained using anti-CD45 allophycocyanin (APC)–Cy7 (530-F11, BioLegend), anti-F4/80 BV421 (BM8, BioLegend), and anti-7/4 phycoerythrin (PE) (AbD Serotec). The myeloid cell populations were gated for CD45 expression and plotted as F4/80 versus 7/4 in FlowJo (V10, Tree Star Inc.).

Endometriosis model

Female BALB/c mice (8 to 12 weeks old) were injected intraperitoneally with pieces of endometrium from syngeneic donor mice (8 to 10 pieces per mouse). These pieces were recovered as lesions from the peritoneum 2 days later. SHA 68R (40 mg/kg, subcutaneously) was given twice daily on the day of inoculation and throughout the experiment. PECs and blood were harvested as described above. The DWB test was done as described earlier (*26*).

Statistical analysis

Unless stated otherwise, the nonparametric Kruskal-Wallis test with Dunn's test for multiple comparisons was used to compare mean values within groups; $P < 0.05$ was deemed significant. Because of additional or missing data points, cytokine data were analyzed using a mixed-effects model, with the Holm-Sidak correction for multiple comparisons. Calculations were performed in Prism V8.1.1 (GraphPad Software Inc.) and SPSS V23 (IBM Corp.).

SUPPLEMENTARY MATERIALS

stm.sciencemag.org/cgi/content/full/13/608/eabd6469/DC1
Materials and Methods
Figs. S1 to S12
Tables S1 to S6
Data file S1
References (*54*–*60*)

View/request a protocol for this paper from *Bio-protocol*.

REFERENCES AND NOTES

1. K. T. Zondervan, C. M. Becker, S. A. Missmer, D. L. Longo, Endometriosis. *N. Engl. J. Med.* **382**, 1244–1256 (2020).
2. S. Simoens, G. Dunselman, C. Dirksen, L. Hummelshoj, A. Bokor, I. Brandes, V. Brodszky, M. Canis, G. L. Colombo, T. DeLeire, T. Falcone, B. Graham, G. Halis, A. Horne, O. Kanj, J. J. Kjer, J. Kristensen, D. Lebovic, M. Mueller, P. Vigano, M. Wullschleger, T. D'Hooghe, The burden of endometriosis: Costs and quality of life of women with endometriosis and treated in referral centres. *Hum. Reprod.* **27**, 1292–1299 (2012).
3. American Society for Reproductive, Revised American Society for Reproductive Medicine classification of endometriosis: 1996. *Fertil. Steril.* **67**, 817–821 (1997).
4. P. Vercellini, L. Fedele, G. Aimi, O. De Giorgi, D. Consonni, P. G. Crosignani, Reproductive performance, pain recurrence and disease relapse after conservative surgical treatment for endometriosis: The predictive value of the current classification system. *Hum. Reprod.* **21**, 2679–2685 (2006).
5. A. Laux-Biehlmann, T. d'Hooghe, T. M. Zollner, Menstruation pulls the trigger for inflammation and pain in endometriosis. *Trends Pharmacol. Sci.* **36**, 270–276 (2015).
6. K. J. Berkley, A. J. Rapkin, R. E. Papka, The pains of endometriosis. *Science* **308**, 1587–1589 (2005).
7. M. Morotti, K. Vincent, C. M. Becker, Mechanisms of pain in endometriosis. *Eur. J. Obstet. Gynecol. Reprod. Biol.* **209**, 8–13 (2017).
8. L. C. Giudice, Clinical practice. Endometriosis. *N. Engl. J. Med.* **362**, 2389–2398 (2010).
9. R. Saha, H. J. Pettersson, P. Svedberg, M. Oloversusson, A. Bergqvist, L. Marions, P. Tornvall, R. Kuja-Halkola, Heritability of endometriosis. *Fertil. Steril.* **104**, 947–952 (2015).
10. K. T. Zondervan, S. A. Treloar, J. Lin, D. E. Weeks, D. R. Nyholt, J. Mangion, I. J. MacKay, L. R. Cardon, N. G. Martin, S. H. Kennedy, G. W. Montgomery, Significant evidence of one or more susceptibility loci for endometriosis with near-Mendelian inheritance on chromosome 7p13–15. *Hum. Reprod.* **22**, 717–728 (2007).
11. J. N. Painter, C. A. Anderson, D. R. Nyholt, S. Macgregor, J. Lin, S. H. Lee, A. Lambert, Z. Z. Zhao, F. Roseman, Q. Guo, S. D. Gordon, L. Wallace, A. K. Henders, P. M. Visscher, P. Kraft, N. G. Martin, A. P. Morris, S. A. Treloar, S. H. Kennedy, S. A. Missmer, G. W. Montgomery, K. T. Zondervan, Genome-wide association study identifies a locus at 7p15.2 associated with endometriosis. *Nat. Genet.* **43**, 51–54 (2011).
12. GTEx Consortium, The Genotype-Tissue Expression (GTEx) project. *Nat. Genet.* **45**, 580–585 (2013).
13. K. T. Zondervan, D. E. Weeks, R. Colman, L. R. Cardon, R. Hadfield, J. Schleffler, A. G. Trainor, C. L. Coe, J. W. Kemnitz, S. H. Kennedy, Familial aggregation of endometriosis in a large pedigree of rhesus macaques. *Hum. Reprod.* **19**, 448–455 (2004).
14. S. A. Treloar, J. Wicks, D. R. Nyholt, G. W. Montgomery, M. Bahlo, V. Smith, G. Dawson, I. J. Mackay, D. E. Weeks, S. T. Bennett, A. Carey, K. R. Ewen-White, D. L. Duffy, D. T. O'Connor, D. H. Barlow, N. G. Martin, S. H. Kennedy, Genomewide linkage study in 1,176 affected sister pair families identifies a significant susceptibility locus for endometriosis on chromosome 10q26. *Am. J. Hum. Genet.* **77**, 365–376 (2005).
15. J. Vendelin, V. Pulkkinen, M. Rehn, A. Pirskanen, A. Räisänen-Sokolowski, A. Laitinen, L. A. Laitinen, J. Kere, T. Laitinen, Characterization of GPRA, a novel G protein–coupled receptor related to asthma. *Am. J. Respir. Cell Mol. Biol.* **33**, 262–270 (2005).
16. L. Sundman, U. Saarialho-Kere, J. Vendelin, K. Lindfors, G. Assadi, K. Kaukinen, M. Westerholm-Ormio, E. Savilahti, M. Mäki, H. Alenius, M. D'Amato, V. Pulkkinen, J. Kere, P. Saavalainen, Neuropeptide S receptor 1 expression in the intestine and skin–putative role in peptide hormone secretion. *Neurogastroenterol. Motil.* **22**, 79–87.e30 (2010).
17. V. Pulkkinen, M.-L. Majuri, G. Wang, P. Holopainen, Y. Obase, J. Vendelin, H. Wolff, P. Rytilä, L. A. Laitinen, T. Haahtela, T. Laitinen, H. Alenius, J. Kere, M. Rehn, Neuropeptide S and G protein-coupled receptor 154 modulate macrophage immune responses. *Hum. Mol. Genet.* **15**, 1667–1679 (2006).
18. J. Gupte, G. Cutler, J.-L. Chen, H. Tian, Elucidation of signaling properties of vasopressin receptor-related receptor 1 by using the chimeric receptor approach. *Proc. Natl. Acad. Sci. U.S.A.* **101**, 1508–1513 (2004).
19. Y. Yao, J. Su, G. Yang, G. Zhang, Z. Lei, F. Zhang, X. Li, R. Kou, Y. Liu, J. Liu, Effects of neuropeptide S on the proliferation of splenic lymphocytes, phagocytosis, and proinflammatory cytokine production of pulmonary alveolar macrophages in the pig. *Peptides* **32**, 118–124 (2011).
20. M. Filaferro, C. Novi, V. Ruggieri, S. Genedani, S. Alboni, D. Malagoli, G. Caló, R. Guerrini, G. Vitale, Neuropeptide S stimulates human monocyte chemotaxis via NPS receptor activation. *Peptides* **39**, 16–20 (2013).
21. N. Okamura, S. A. Habay, J. Zeng, A. R. Chamberlin, R. K. Reinscheid, Synthesis and pharmacological in vitro and in vivo profile of 3-oxo-1,1-diphenyl-tetrahydro-oxazolo[3,4-a]pyrazine-7-carboxylic acid 4-fluoro-benzylamide (SHA 68), a selective antagonist of the neuropeptide S receptor. *J. Pharmacol. Exp. Ther.* **325**, 893–901 (2008).
22. R. K. Reinscheid, Y.-L. Xu, N. Okamura, J. Zeng, S. Chung, R. Pai, Z. Wang, O. Civelli, Pharmacological characterization of human and murine neuropeptide S receptor variants. *J. Pharmacol. Exp. Ther.* **315**, 1338–1345 (2005).
23. R. Guerrini, S. Salvadori, A. Rizzi, D. Regoli, G. Calo, Neurobiology, pharmacology, and medicinal chemistry of neuropeptide S and its receptor. *Med. Res. Rev.* **30**, 751–777 (2010).
24. E. R. Wendt, H. Ferry, D. R. Greaves, S. Keshav, Ratiometric analysis of fura red by flow cytometry: A technique for monitoring intracellular calcium flux in primary cell subsets. *PLOS ONE* **10**, e0119532 (2015).
25. J. L. Cash, G. E. White, D. R. Greaves, *Methods in Enzymology* (Elsevier, 2009), pp. 379–396.
26. A. Laux-Biehlmann, J. Boyken, H. Dahllöf, N. Schmidt, T. M. Zollner, J. Nagel, Dynamic weight bearing as a non-reflexive method for the measurement of abdominal pain in mice. *Eur. J. Pain* **20**, 742–752 (2016).

27. K. Zondervan, N. Rahmioglu, A. Morris, D. Nyholt, G. Montgomery, C. Becker, S. Missmer, Beyond endometriosis genome-wide association study: From genomics to phenomics to the patient. *Semin. Reprod. Med.* **34**, 242–254 (2016).
28. A. Moshiri, R. Chen, S. Kim, R. A. Harris, Y. Li, M. Raveendran, S. Davis, Q. Liang, O. Pomerantz, J. Wang, L. Garzel, A. Cameron, G. Yiu, J. T. Stout, Y. Huang, C. J. Murphy, J. Roberts, K. N. Gopalakrishna, K. Boyd, N. O. Artemyev, J. Rogers, S. M. Thomasy, A nonhuman primate model of inherited retinal disease. *J. Clin. Invest.* **129**, 863–874 (2019).
29. B. K. Dray, M. Raveendran, R. A. Harris, F. Benavides, S. B. Gray, C. J. Perez, M. J. McArthur, L. E. Williams, W. B. Baze, H. Doddapaneni, D. M. Muzny, C. R. Abee, J. Rogers, Mismatch repair gene mutations lead to lynch syndrome colorectal cancer in rhesus macaques. *Genes Cancer* **9**, 142–152 (2018).
30. T. Laitinen, A. Polvi, P. Rydman, J. Vendelin, V. Pulkkinen, P. Salmikangas, S. Mäkelä, M. Rehn, A. Pirskanen, A. Rautanen, M. Zucchelli, H. Gullstén, M. Leino, H. Alenius, T. Petäys, T. Haahtela, A. Laitinen, C. Laprise, T. J. Hudson, L. A. Laitinen, J. Kere, Characterization of a common susceptibility locus for asthma-related traits. *Science* **304**, 300–304 (2004).
31. N. Acevedo, S. Ezer, S. Kebede Merid, V. D. Gaertner, C. Söderhäll, M. D'Amato, M. Kabesch, E. Melén, J. Kere, V. Pulkkinen, Neuropeptide S (NPS) variants modify the signaling and risk effects of NPS Receptor 1 (NPSR1) variants in asthma. *PLOS ONE* **12**, e0176568 (2017).
32. G. Malerba, C. M. Lindgren, L. Xumerle, P. Kiviluoma, E. Trabetti, T. Laitinen, R. Galavotti, L. Pescollderungg, A. L. Boner, J. Kere, P. F. Pignatti, Chromosome 7p linkage and GPR154 gene association in Italian families with allergic asthma. *Clin. Exp. Allergy* **37**, 83–89 (2007).
33. C. Vergara, S. Jiménez, N. Acevedo, B. Martínez, D. Mercado, L. Gusmão, N. Rafaels, T. Hand, K. C. Barnes, L. Caraballo, Association of G-protein-coupled receptor 154 with asthma and total IgE in a population of the Caribbean coast of Colombia. *Clin. Exp. Allergy* **39**, 1558–1568 (2009).
34. M. D'Amato, S. Bruce, F. Bresso, M. Zucchelli, S. Ezer, V. Pulkkinen, C. Lindgren, M. Astegiano, M. Rizzetto, P. Gionchetti, G. Riegler, R. Sostegni, M. Daperno, S. D'Alfonso, P. Momigliano-Richiardi, L. Torkvist, P. Puolakkainen, M. Lappalainen, P. Paavola-Sakki, L. Halme, M. Farkkila, U. Turunen, K. Kontula, R. Lofberg, S. Pettersson, J. Kere, Neuropeptide S receptor 1 gene polymorphism is associated with susceptibility to inflammatory bowel disease. *Gastroenterology* **133**, 808–817 (2007).
35. M. D'Amato, M. Zucchelli, M. Seddighzadeh, F. Anedda, S. Lindblad, J. Kere, L. Alfredsson, L. Klareskog, L. Padyukov, Analysis of neuropeptide S receptor gene (NPSR1) polymorphism in rheumatoid arthritis. *PLOS ONE* **5**, e9315 (2010).
36. N. Okamura, K. Hashimoto, M. Iyo, E. Shimizu, A. Dempfle, S. Friedel, R. K. Reinscheid, Gender-specific association of a functional coding polymorphism in the Neuropeptide S receptor gene with panic disorder but not with schizophrenia or attention-deficit/hyperactivity disorder. *Prog. Neuropsychopharmacol. Biol. Psychiatry* **31**, 1444–1448 (2007).
37. R. Kumsta, F. S. Chen, H.-C. Pape, M. Heinrichs, Neuropeptide S receptor gene is associated with cortisol responses to social stress in humans. *Biol. Psychol.* **93**, 304–307 (2013).
38. K. A. Raczka, N. Gartmann, M.-L. Mechias, A. Reif, C. Büchel, J. Deckert, R. Kalisch, A neuropeptide S receptor variant associated with overinterpretation of fear reactions: A potential neurogenetic basis for catastrophizing. *Mol. Psychiatry* **15**, 1067–1074 (2010).
39. M. Henström, M. Zucchelli, C. Söderhäll, A. Bergström, J. Kere, E. Melén, O. Olén, M. D'Amato, *NPSR1* polymorphisms influence recurrent abdominal pain in children: A population-based study. *Neurogastroenterol. Motil.* **26**, 1417–1425 (2014).
40. F. Anedda, M. Zucchelli, D. Schepis, A. Hellquist, L. Corrado, S. D'Alfonso, A. Achour, G. McInerney, A. Bertorello, M. Lördal, R. Befrits, J. Björk, F. Bresso, L. Törkvist, J. Halfvarson, J. Kere, M. D'Amato, Multiple polymorphisms affect expression and function of the neuropeptide S receptor (NPSR1). *PLOS ONE* **6**, e29523 (2011).
41. I. Tracey, P. W. Mantyh, The cerebral signature for pain perception and its modulation. *Neuron* **55**, 377–391 (2007).
42. M. R. Nelson, H. Tipney, J. L. Painter, J. Shen, P. Nicoletti, Y. Shen, A. Floratos, P. C. Sham, M. J. Li, J. Wang, L. R. Cardon, J. C. Whittaker, P. Sanseau, The support of human genetic evidence for approved drug indications. *Nat. Genet.* **47**, 856–860 (2015).
43. E. Greaves, F. L. Cousins, A. Murray, A. Esnal-Zufiaurre, A. Fassbender, A. W. Horne, P. T. K. Saunders, A novel mouse model of endometriosis mimics human phenotype and reveals insights into the inflammatory contribution of shed endometrium. *Am. J. Pathol.* **184**, 1930–1939 (2014).
44. K. T. Zondervan, C. M. Becker, K. Koga, S. A. Missmer, R. N. Taylor, P. Viganò, Endometriosis. *Nat. Rev. Dis. Primers.* **4**, 9 (2018).
45. V. Pulkkinen, R. Haataja, U. Hannelius, O. Helve, O. M. Pitkänen, R. Karikoski, M. Rehn, R. Marttila, C. M. Lindgren, J. Hästbacka, S. Andersson, J. Kere, M. Hallman, T. Laitinen, G protein-coupled receptor for asthma susceptibility associates with respiratory distress syndrome. *Ann. Med.* **38**, 357–366 (2006).
46. J. Vendelin, S. Bruce, P. Holopainen, V. Pulkkinen, P. Rytilä, A. Pirskanen, M. Rehn, T. Laitinen, L. A. Laitinen, T. Haahtela, U. Saarialho-Kere, A. Laitinen, J. Kere, Downstream target genes of the neuropeptide S–NPSR1 pathway. *Hum. Mol. Genet.* **15**, 2923–2935 (2006).
47. A. Fassbender, N. Rahmioglu, A. F. Vitonis, P. Viganò, L. C. Giudice, T. M. D'Hooghe, L. Hummelshoj, G. D. Adamson, C. M. Becker, S. A. Missmer, K. T. Zondervan, G. D. Adamson, C. Allaire, R. Anchan, C. M. Becker, M. A. Bedaiwy, G. M. B. Louis, C. Calhaz-Jorge, K. Chwalisz, T. M. D'Hooghe, A. Fassbender, T. Faustmann, A. T. Fazleabas, I. Flores, A. Forman, I. Fraser, L. C. Giudice, M. Gotte, P. Gregersen, S.-W. Guo, T. Harada, D. Hartwell, A. W. Horne, M. L. Hull, L. Hummelshoj, M. G. Ibrahim, L. Kiesel, M. R. Laufer, K. Machens, S. Mechsner, S. A. Missmer, G. W. Montgomery, A. Nap, M. Nyegaard, K. G. Osteen, C. A. Petta, N. Rahmioglu, S. P. Renner, J. Riedlinger, S. Roehrich, P. A. Rogers, L. Rombauts, A. Salumets, E. Saridogan, T. Seckin, P. Stratton, K. L. Sharpe-Timms, S. Tworoger, P. Vigano, K. Vincent, A. F. Vitonis, U.-H. Wienhues-Thelen, P. P. Yeung, P. Yong, K. T. Zondervan; WERF EPHect Working Group, World Endometriosis Research Foundation Endometriosis Phenome and Biobanking Harmonisation Project: IV. Tissue collection, processing, and storage in endometriosis research. *Fertil. Steril.* **102**, 1244–1253 (2014).
48. G. R. Abecasis, S. S. Cherny, W. O. Cookson, L. R. Cardon, Merlin–rapid analysis of dense genetic maps using sparse gene flow trees. *Nat. Genet.* **30**, 97–101 (2002).
49. E. Sobel, H. Sengul, D. E. Weeks, Multipoint estimation of identity-by-descent probabilities at arbitrary positions among marker loci on general pedigrees. *Hum. Hered.* **52**, 121–131 (2001).
50. N. Rahmioglu, A. W. Drong, H. Lockstone, T. Tapmeier, K. Hellner, M. Saare, T. Laisk-Podar, C. Dew, E. Tough, G. Nicholson, M. Peters, A. P. Morris, C. M. Lindgren, C. M. Becker, K. T. Zondervan, Variability of genome-wide DNA methylation and mRNA expression profiles in reproductive and endocrine disease related tissues. *Epigenetics* **12**, 897–908 (2017).
51. M. W. Pfaffl, A new mathematical model for relative quantification in real-time RT-PCR. *Nucleic Acids Res.* **29**, 45e (2001).
52. C. Trapella, M. Pela, L. Del Zoppo, G. Calo, V. Camarda, C. Ruzza, A. Cavazzini, V. Costa, V. Bertolasi, R. K. Reinscheid, S. Salvadori, R. Guerrini, Synthesis and separation of the enantiomers of the neuropeptide S receptor antagonist (9R/S)-3-Oxo-1,1-diphenyl-tetrahydro-oxazolo[3,4-a]pyrazine-7-carboxylic acid 4-fluoro-benzylamide (SHA 68). *J. Med. Chem.* **54**, 2738–2744 (2011).
53. C. O. Pietras, J. Vendelin, F. Anedda, S. Bruce, M. Adner, L. Sundman, V. Pulkkinen, H. Alenius, M. D'Amato, C. Söderhäll, J. Kere, The asthma candidate gene *NPSR1* mediates isoform specific downstream signalling. *BMC Pulm. Med.* **11**, 39 (2011).
54. J. Gayán, D. Brocklebank, J. M. Andresen, G. Alkorta-Aranburu; US-Venezuela Collaborative Research Group, M. Zameel Cader, S. A. Roberts, S. S. Cherny, N. S. Wexler, L. R. Cardon, D. E. Housman, Genomewide linkage scan reveals novel loci modifying age of onset of Huntington's disease in the Venezuelan HD kindreds. *Genet. Epidemiol.* **32**, 445–453 (2008).
55. D. R. Zerbino, P. Achuthan, W. Akanni, M. R. Amode, D. Barrell, J. Bhai, K. Billis, C. Cummins, A. Gall, C. G. Girón, L. Gil, L. Gordon, L. Haggerty, E. Haskell, T. Hourlier, O. G. Izuogu, S. H. Janacek, T. Juettemann, J. K. To, M. R. Laird, I. Lavidas, Z. Liu, J. E. Loveland, T. Maurel, W. McLaren, B. Moore, J. Mudge, D. N. Murphy, V. Newman, M. Nuhn, D. Ogeh, C. K. Ong, A. Parker, M. Patricio, H. S. Riat, H. Schuilenburg, D. Sheppard, H. Sparrow, K. Taylor, A. Thormann, A. Vullo, B. Walts, A. Zadissa, A. Frankish, S. E. Hunt, M. Kostadima, N. Langridge, F. J. Martin, M. Muffato, E. Perry, M. Ruffier, D. M. Staines, S. J. Trevanion, B. L. Aken, F. Cunningham, A. Yates, P. Flicek, Ensembl 2018. *Nucleic Acids Res.* **46**, D754–D761 (2018).
56. M. Haeussler, A. S. Zweig, C. Tyner, M. L. Speir, K. R. Rosenbloom, B. J. Raney, C. M. Lee, B. T. Lee, A. S. Hinrichs, J. N. Gonzalez, D. Gibson, M. Diekhans, H. Clawson, J. Casper, G. P. Barber, D. Haussler, R. M. Kuhn, W. J. Kent, The UCSC Genome Browser database: 2019 update. *Nucleic Acids Res.* **47**, D853–D858 (2019).
57. A. Suzuki, S. Kawano, T. Mitsuyama, M. Suyama, Y. Kanai, K. Shirahige, H. Sasaki, K. Tokunaga, K. Tsuchihara, S. Sugano, K. Nakai, Y. Suzuki, DBTSS/DBKERO for integrated analysis of transcriptional regulation. *Nucleic Acids Res.* **46**, D229–D238 (2018).
58. Z. Z. Zhao, D. R. Nyholt, L. Le, N. G. Martin, M. R. James, S. A. Treloar, G. W. Montgomery, KRAS variation and risk of endometriosis. *Mol. Hum. Reprod.* **12**, 671–676 (2006).
59. K. Fukatsu, Y. Nakayama, N. Tarui, M. Mori, H. Matsumoto, O. Kurasawa, H. Banno, Bicyclic piperazine compound and use thereof, patent no. WO2005021555A1 (2005).
60. E. D. Amir, K. L. Davis, M. D. Tadmor, E. F. Simonds, J. H. Levine, S. C. Bendall, D. K. Shenfeld, S. Krishnaswamy, G. P. Nolan, D. Pe'er, viSNE enables visualization of high dimensional single-cell data and reveals phenotypic heterogeneity of leukemia. *Nat. Biotechnol.* **31**, 545–552 (2013).

Acknowledgments: We wish to thank all the women who participated in our studies and who donated samples to our research. We would like to thank C. Hubbard, K. Barrett, M. Dale, and C. Dew of the Oxford Endometriosis CaRe Centre, University of Oxford, UK. We also thank R. Gibbs, D. Muzny, and the staff of the Baylor Human Genome Sequencing Center, Baylor College of Medicine, USA, as well as the clinical veterinarians and pathology staff of the Wisconsin National Primate Research Center. **Funding:** The

genetic analyses were supported by multiple Wellcome Trust grants to K.T.Z. (084766/Z/08/Z, 085235/Z/08/Z, and 085235/Z/08/A). The rhesus macaque microsatellite and DNA sequencing work was funded by NIH grants R29-RR08781 and R24-OD011173 to J.R., and by internal funds from the Baylor College of Medicine. The in vitro and in vivo work was supported by the Alliance of the University of Oxford and Bayer AG Pharmaceuticals on Novel Targets for Gynecological Therapies. **Author contributions:** Conceptualization: T.T.T., N.R., J.L., C.M.B., U.O., T.M.Z., S.H.K., J.W.K., J.R., and K.T.Z.; data curation: T.T.T., N.R., J.L., B.D.L., M.O., C.B., D.B., M.G., R.A.H., E.L., G.L., J.M., S. Manek, N.G.M., G.W.M., H.A.S., S.T., G.W., S.H.K., and K.T.Z.; formal analysis: T.T.T., N.R., J.L., D.B., R.A.H., and K.T.Z.; funding acquisition: H.H.-S., C.M.B., U.O., T.M.Z., S.H.K., J.W.K., J.R., and K.T.Z.; investigation: T.T.T., N.R., J.L., B.D.L., M.O., M.R., C.B., M.G., R.A.H., A.L.-B., J.M., N.G.M., F.O.M., S. Mesch, G.W.M., H.A.S., S.T., and G.W.; methodology: T.T.T., N.R., J.L., B.D.L., R.A.H., E.L., G.L., F.O.M., A.P.M., J.N., and J.R.; project administration: T.T.T., O.M.F., H.H.-S., C.S., C.M.B., U.O., T.M.Z., and K.T.Z.; resources: M.R., G.W.M., H.A.S., C.M.B., U.O., T.M.Z., S.H.K., J.W.K., J.R., and K.T.Z.; software: T.T.T. and N.R.; supervision: T.T.T., O.M.F., C.M.B., U.O., T.M.Z., S.H.K., J.W.K., J.R., and K.T.Z.; visualization: T.T.T., N.R., and J.L.; writing—original draft: T.T.T., N.R., J.R., and K.T.Z.; writing—review and editing: all authors. **Competing interests:** B.D.L., M.O., O.M.F., H.H.-S., A.L.-B., S. Mesch, J.N., and T.M.Z. are employees and shareholders of Bayer AG Pharmaceuticals. K.T.Z. and C.M.B. have research collaborations through the University of Oxford in benign gynecology with Bayer AG, Roche Diagnostics, Volition UK, and M DNA Life Sciences. **Data and materials availability:** All data associated with this study are present in the paper or the Supplementary Materials.

Submitted 3 July 2020
Resubmitted 25 February 2021
Accepted 6 August 2021
Published 25 August 2021
10.1126/scitranslmed.abd6469

Citation: T. T. Tapmeier, N. Rahmioglu, J. Lin, B. De Leo, M. Obendorf, M. Raveendran, O. M. Fischer, C. Bafligil, M. Guo, R. A. Harris, H. Hess-Stumpp, A. Laux-Biehlmann, E. Lowy, G. Lunter, J. Malzahn, N. G. Martin, F. O. Martinez, S. Manek, S. Mesch, G. W. Montgomery, A. P. Morris, J. Nagel, H. A. Simmons, D. Brocklebank, C. Shang, S. Treloar, G. Wells, C. M. Becker, U. Oppermann, T. M. Zollner, S. H. Kennedy, J. W. Kemnitz, J. Rogers, K. T. Zondervan, Neuropeptide S receptor 1 is a nonhormonal treatment target in endometriosis. *Sci. Transl. Med.* **13**, eabd6469 (2021).

Science Translational Medicine

Neuropeptide S receptor 1 is a nonhormonal treatment target in endometriosis

Thomas T. Tapmeier, Nilufer Rahmioglu, Jianghai Lin, Bianca De Leo, Maik Obendorf, Muthuswamy Raveendran, Oliver M. Fischer, Cemsel Bafligil, Manman Guo, Ronald Alan Harris, Holger Hess-Stumpp, Alexis Laux-Biehlmann, Ernesto Lowy, Gerton Lunter, Jessica Malzahn, Nicholas G. Martin, Fernando O. Martinez, Sanjiv Manek, Stefanie Mesch, Grant W. Montgomery, Andrew P. Morris, Jens Nagel, Heather A. Simmons, Denise Brocklebank, Catherine Shang, Susan Treloar, Graham Wells, Christian M. Becker, Udo Oppermann, Thomas M. Zollner, Stephen H. Kennedy, Joseph W. Kemnitz, Jeffrey Rogers and Krina T. Zondervan

Sci Transl Med **13**, eabd6469.
DOI: 10.1126/scitranslmed.abd6469

Abolishing endometriosis inflammation

Endometriosis is a condition where endometrial-like tissues grow outside the uterus, leading to inflammation, pain, and reduced fertility. Treatment is generally hormonal or surgical, and noninvasive, nonhormonal therapies are urgently needed. Here, Tapmeier and colleagues performed genetic analyses of human families with endometriosis and rhesus macaques that spontaneously develop endometriosis, identifying *NPSR1*, the gene encoding neuropeptide S receptor 1, as associated with disease. The NPSR1 inhibitor SHA 68R led to reduction of inflammatory cell infiltrate and pain in mouse models of peritoneal inflammation and endometriosis. Although further studies in nonhuman primates are needed, the findings give hope for a nonhormonal treatment for endometriosis.